IJSRM
INTERNATIONAL JOURNAL OF SCIENCE AND RESEARCH METHODOLOGY
An Official Publication of Human Journals

Human Journals
Research Article
November 2016 Vol.:5, Issue:1

Thermal and Non-Thermal Microwave Absorption in Long Bone

IJSRM
INTERNATIONAL JOURNAL OF SCIENCE AND RESEARCH METHODOLOGY
An Official Publication of Human Journals

Mona A. El Naggar*, Medhat A. Messiery

Engineering Physics and Maths. Dept., Fac. of Engineering, Cairo University, Egypt.

Submission: 2 November 2016
Accepted: 7 November 2016
Published: 25 November 2016

HUMAN JOURNALS

www.ijsrm.humanjournals.com

Keywords: Mathematical Model, Dissipated Power Density, Stored Power density, Cortical Bone, Bone marrow, Microwave exposure, EMF radiation, EMF strengths, Frequency dependence

ABSTRACT

The present work introduces a mathematical model, based on Maxwell's equations, to trace the penetration of EMF within the frequency range (1MHz-10GHZ) through long bone and bone marrow. The mathematical model is employed with special emphasis on the real and imaginary components of power absorbed. This model adopts the current reported electromagnetic properties to produce the complex permittivity, reflection and transmission coefficients. The model calculates the amount of dissipated power and that stored due to far field microwave exposure to electric field (1V/m-2kV/m). The results obtained are compared to the accepted standards of safety limits. Accordingly, for electric field strengths less than 2kV/m and frequency 10GHz, the power absorbed is within the reported standards. However, both tissues store a considerable amount of power density which could lead to thermal and non-thermal effects.

1. INTRODUCTION

Recently, the indispensable microwave applications have been intensified the level of environmental electromagnetic radiation. The assessment of its biological effects has become a wide field of research [1-5]. This is hindered, firstly by the lack of accurate data for the biological properties, secondly by the difficulties in assessing the whole body radiation exposure. Thirdly, the human response to microwave exposure is diverse and still a potent source of controversy.

The specific absorption rate (SAR), is the most acknowledged quantity for international standardization. These assessments are implemented by animal experimentations [6, 7], phantom model measurements [8-11] and mathematical approaches. The latter employs either deterministic mathematical derivations [12-15], stochastic modeling [16], or computer simulations [17].

The aim of the current study is to introduce an analytical approach to calculate the average power density absorbed, both stored and dissipated, within cortical bone and bone marrow. Hence, the produced results are analyzed in the light of thermal and non- thermal biological effects.

2. MATHEMATICAL METHODOLOGY

The present work is an extension of a previous model introduced by the author M. A. El-Naggar[14]. This model employs is a mathematical one that traces the far field microwave propagation through long bone. Maxwell's equations are employed and the reported physical electromagnetic properties of cortical bone and bone marrow, [18-24], are implemented. The model assumes the incidence of an electromagnetic wave on a homogeneous multilayer long bone section (bone-marrow-bone). Assuming the wave propagates along the normal direction to the sample surface (x-direction), the electric field component is along the y-direction of strengths (1V/m-2kV/m) and frequency varying in the range (1MHz-10GHz). A bone sample of 1mm^2 surface area, consisting of 3mm thickness cortical bone within which a 5mm bone marrow lies, is assumed. The average power density is calculated for both the cortical bone, P_{bone}, and the marrow, P_{marrow}, in the frequency range assumed for the different electric field strengths. The reflection on successive interfaces contributes to the overall calculated power.

The electrical and magnetic properties of the media are considered as complex functions of frequency, namely; permittivity, $\varepsilon(f)$, conductivity, $\sigma(f)$, and permeability, $\mu(f)$.
The average power density P_{avei} ,is calculated for the i[th] layer as:

$$P_{avei} = \frac{1}{\Delta xi}\int_0^{\Delta xi}\frac{1}{T}\sqrt{\left\{\int_0^T\{P_{xi}(x,t)\}^2dt\right\}}\,dx \qquad (1)$$

$$P_{xi}(x,t) = E_{yi}(x,t)\times H_{zi}(x,t) \quad (2)$$

Mathematical analysis calculates the electric and magnetic field distributions in the three consecutive layers. The detailed mathematical analysis is given in Appendix 1.

3. RESULTS

Computations are performed using Maple-V software. The program computes the total electric and magnetic fields and the power absorbed (both dissipated, P_{diss}, and that stored, P_{str} in respective layers. Horizontally polarized EM fields are assumed to be normally incident. Hence, the power density function is calculated in w/m$^{2.}$ Figures (1-a,1-b) illustrate the variation of power density, both dissipated and stored versus the frequency, in log scale, for electric field strengths ranging; 1V/m-100V/m.

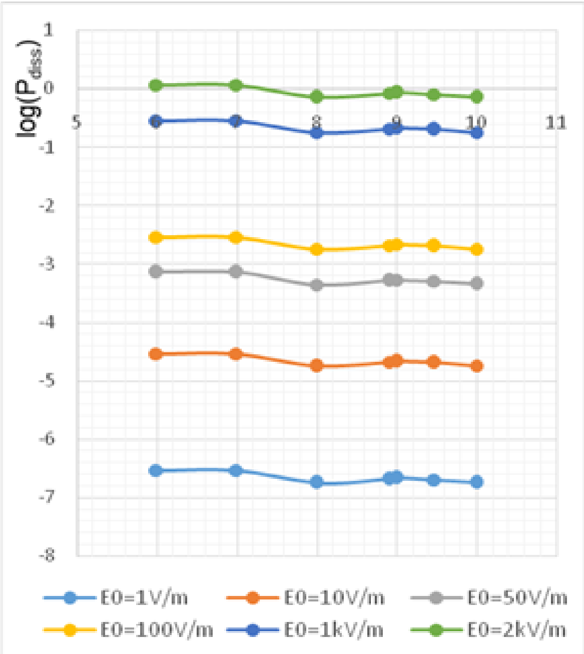

Fig.1-a log(Pdiss) vs log(f) within the cortical bone layer

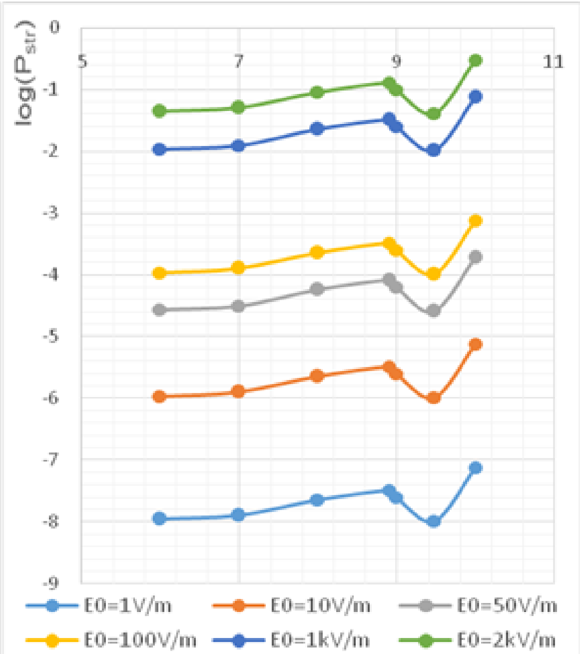

Fig.1-b log(Pstr) vs log(f) within the cortical bone layer

Figures (2-a, 2-b) represent the distribution of the power density, both dissipated and stored in the marrow layer versus frequency, in log scale. Figure 3 shows the distribution of the power density ratio of that absorbed in the marrow layer to that absorbed in the bone layer, in dB, versus log(f).

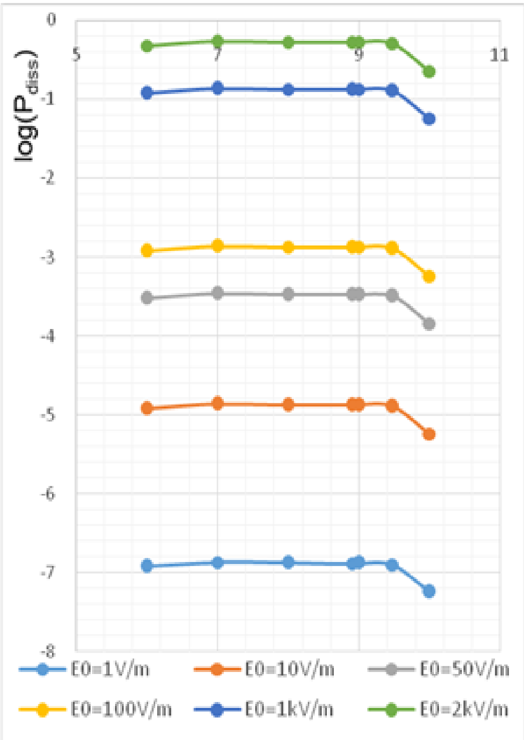

Fig.2-a log(Pdiss) vs log(f) within the bone marrow

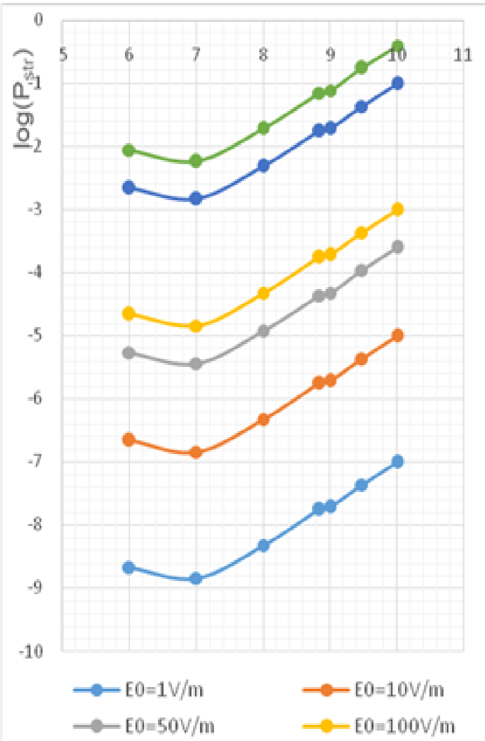

Fig.2-b log(Pstr) vs log (f) within the bone marrow

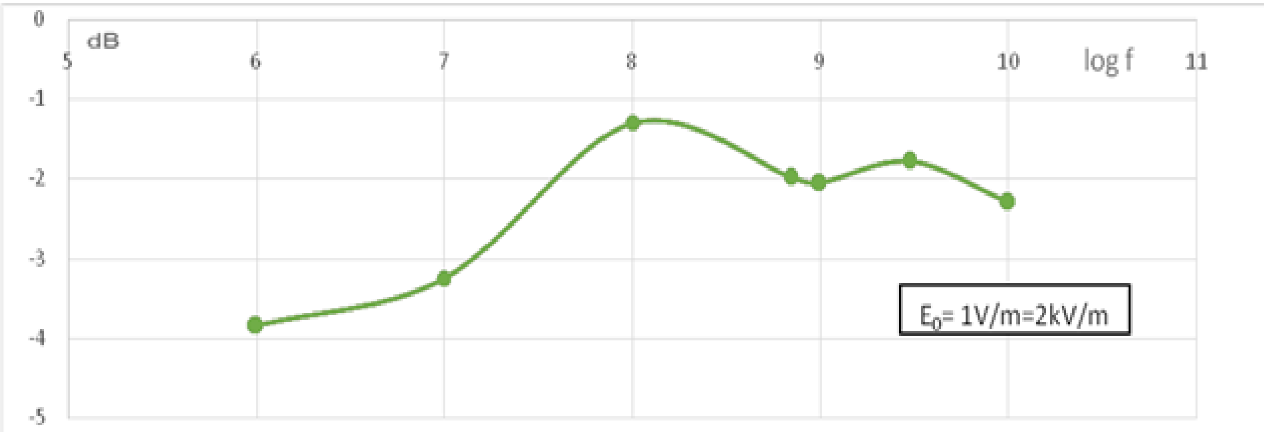

Fig.3.10log(P_{marrow}/P_{bone}) vs log(f) and $E_0$for bone for normal incidence

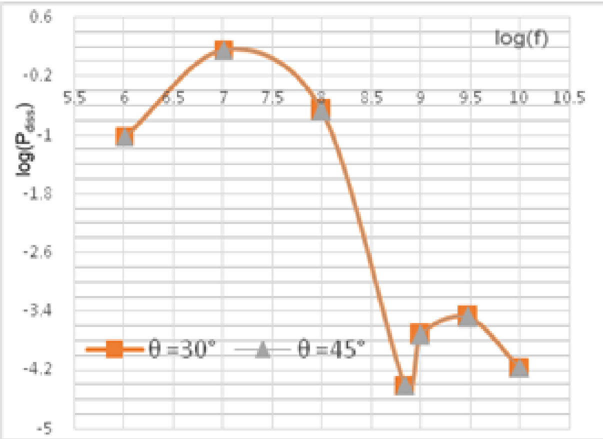

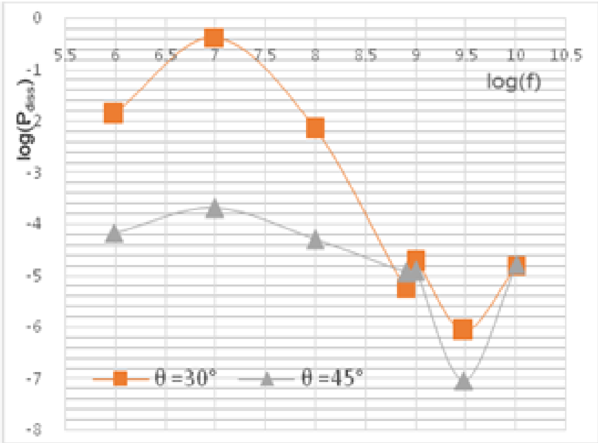

Fig.4-a log(Pdiss) vs log(f) for bone calculated for E_0=50V/m with different incidence angles

Fig.4-b log(Pstr) vs log(f) for bone calculated for E_0=50V/m with different incidence angles

In the case of oblique incidence, at angles 30^0 and 45^0, on cortical bone, figures (4-a, 4-b) illustrate the rise of power density dissipated and that absorbed versus frequency, in log scale, for electric field strength 50 V/m. Figures (5-a, 5-b) illustrate the rise of power density dissipated and absorbed, versus frequency, in log scale, for electric field strengths 50 V/m for bone marrow in case of oblique incidence for the same angles.

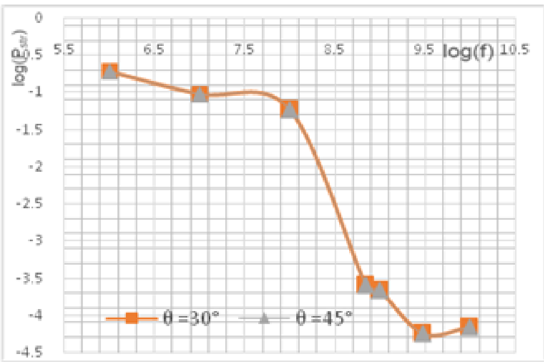

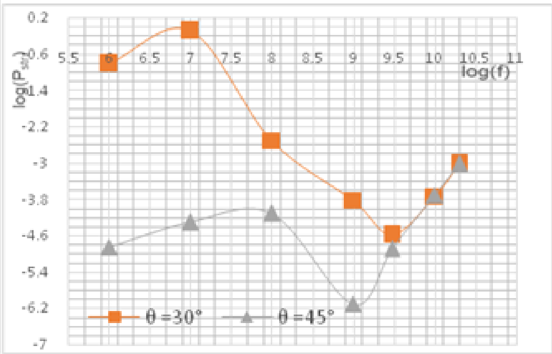

Fig.5-a log(P_{diss}) vs log(f) for marrow calculated for E_0=50V/m with different incidence angles

Fig.5-b log(P_{strd}) vs log(f) for marrow calculated for E_0=50V/m with different incidence angles

4. DISCUSSION

The main aim of the present work is to build up a mathematical model to calculate the power dissipated and stored in bone and bone marrow due to environmental electromagnetic exposure. Hence the results obtained can be compared with the international safety standards. The frequency range, (1MHz-10GHz), is chosen within that employed by most applications e.g. Wi-Fi, Bluetooth, mobile antenna, etc. The electric field exposure is taken to comply with its average values emitted by these sources (1V/m-2KV/m). The present calculations considered the complex nature of the dielectric constant and its relation to the dissipated and stored power density in both cortical bone and bone marrow. Fig.1a shows that the dissipated power density is not significantly frequency dependent whereas it considerably increases with the increase of incident electric field. Similar behavior is observed with the stored power density, fig.1b, with a noticeable valley at frequency range (2GHz-3GHz) which is consistent with all chosen electric field values. On the other hand, the stored power density distribution, in bone marrow, exhibit a rise at frequencies higher than 100MHz (fig. 2b). Fig 3 shows the variation of the relative average power density absorbed in marrow to that in bone, expressed in dB, with the frequency. The relation exhibits a peak at 100MHz and a valley around the frequencies (900MHz-3GHz).

In the above figures the electromagnetic field is assumed to be normally incident on bone sample. As the angle of incidence varies (30° and 45°) fig.4a and fig.4b show the effect on both dissipated and stored power density as calculated at 50v/m. Considering that the present work analysis adopts the TM mode, it is noteworthy that there is no apparent effect observed on the power density as incidence angle changes in this range,. For marrow, similar figures are produced (fig.5a, fig.5b); dissipated power density exhibits a peak at frequency 10MHz and a minimum at 2.5GHZ, and almost similar behavior is reported for the stored power density.

5. CONCLUSION

According to the present work, thermal effects are accounted for by the real component of the average electromagnetic power absorbed in biological tissue, whereas the non-thermal effects are accounted for by the imaginary component.From the results produced here, we conclude that the far-field exposure caused by electromagnetic pollution would possibly produce power density in cortical bone and marrow that is still within the permissible ranges of public exposure[25-28].Table 1 illustrates both the present work values and international standards. The values obtained are still lower than the international safety standards providing that the electric field strength doesn't exceed 2Kv/m and frequency 10GHz.The dissipated power density in the marrow, believed to be the main source of thermal effect, depends on both the incident electric field and its frequency, with a little dependence on the angle of incidence.

The present work shows the importance of the power stored in both bone and bone marrow. We believe that this power is responsible for the non-thermal effects that are still a main source of debate. Unfortunately, there are no reported safety guidelines for these effects.

It is noteworthy that the validity of the present model depends on the physical electromagnetic constants of both cortical bone and bone marrow. During the preliminary work, we concluded that the skin effect for both bone and marrow is insignificant, as far as the power dissipated or stored is concerned. However, the power penetration depends on the thickness of each layer. Particular concern should be given to the children under the age of five, whose bones are relatively thin with different electromagnetic properties than adults. This makes them vulnerable to harmful effects due to microwave exposure.

Table 1. Illustration of the present work values and the international standards.

Establishment	Exposure	Frequency (Hz)	Permissible Limits (W/m^2)		Present Work(W/m^2) (calculated at 2Kv/m)			
					Bone		Marrow	
					P_{diss}	P_{str}	P_{diss}	P_{str}
ICNIRP [26,27]	Public	900M	4.5		0.82965	0.12941	0.52706	0.07041
		1.8G	9		0.85866	0.10047	0.53214	0.07677
		2.45G	10		0.80956	0.03407	0.50836	0.17563
	Occupational	900M	22.5		----	----	----	----
		1.8G	45					
		2.45G	--					
WHO[28]	Public	10M-10G	Head	4	1.15296 - 0.71769	0.05014 - .30046	0.5458 - 0.2287	0.0058- 0.3969
			Limb	10				
	Occupational	10M-10G	Head	20	-----	-----	-----	----
			Limb	50				

REFERENCES

1. Foster R., Thermal and Non-thermal Mechanisms of Interaction of Radio-Frequency Energy with Biological Systems. Feb 2000, IEEE Transactions on Plasma Science, 28(1).

2. Cleary S.F. Cao G. Liu L-M. Effects of isothermal 2.45 GHz microwave radiation on the mammalian cell cycle: Comparison with effects of isothermal 27 MHz radiofrequency radiation exposure. Bioelectrochem. Bioeneng. 39: 1996, 167-173.
3. Stuchly M. A. Fundamentals of the Interactions of Radio-frequency and Microwave Energies with Matter. Biological effects and dosimetry of nonionizing radiation, RF and microwave energies; NATO advanced study institutes series, Plenum Press, NY, 1983.
4. Repacholi M. H. Low-Level Exposure to Radiofrequency Electromagnetic Fields: Health Effects and Research Needs. Bioelectromagnetics. 1998, (19) 1–19.
5. Jenn D., Electromagnetic Radiation Hazards, *Naval Postgraduate School Department of Electrical & Computer Engineering Monterey, California, EC3630 Radiowave Propagation*
6. Zhong C. Zhang X. Xu Z.He R. Effects of low-intensity electromagnetic fields on the proliferation and differentiation of cultured mouse bone marrow stromal cells, Phys. Ther.;92(9):1208-19. doi: 10.2522/ptj.20110224. Sept. 2012, Epub,
7.Prisco M. G. Nasta F. Rosado M. M. Lovisolo G. A. Marino C. Pioli C. Effects of GSM-modulated radiofrequency electromagnetic fields on mouse bone marrow cells. Radiat Res.;. doi: 10.1667/RR1213.1, 170(6): Dec 2008, 803-810.
8. Gosselin M. C. Joseph W. et al. Estimation Formulas for the Specific Absorption Rate in Humans Exposed to Base-Station Antennas. IEEE Transactions on Electromagnetic Compatibility. 2011.
9. Buleandra Alina, Petrescu Teodor. Comparison of specific absorption rates induced in a model of the human skull. U.P.B. Sci. Bull., series C, (73), Issue1, 2011, 83-92.
10. Yusoff N.I.M., Khatun S., Alshehri S.A. Characterization of absorption loss for UWB body tissue propagation model, Proceedings of the 2009 IEEE 9th Malaysia International Conference on Communications, 2009.
11. Christ A., Klingenbock A., Samaras T., Goiceanu C. and Kuster N. The Dependence of Electromagnetic Far-Field Absorption on Body Tissue Composition in the Frequency Range from 300MHz to 6GHz., IEEE Transactions on microwave theory and techniques, vol. 54, No.5,May 2006, 2188-2194.
12. Gajšek P. D'Andrea J. A. Mason P. A. ZiriaxJ. M. Walters T. J. Hurt W. D Meyer F. J. C. Jakobus U. Samaras T. Sahalos J. N. Mathematical Modeling of EMF Energy Absorption in Biological Systems. Biological Effects of Electromagnetic Fields, 2003, 114-141.
13. El Naggar M. A. El Messiery M. A. Evaluation of power absorption in human eye tissue. International Journal of Advanced Research, Journal homepage: http:// www.journalijar.com, (1), Issue 7, ISSN 2320-5407, 2013,658-665...
14. El Naggar M. A. EMF Power Absorption in Bone and Bone Marrow: Mathematical Model. 2015, 7 (1):, Articleno.PSIJ2015.053, SCIENCE-DOMAIN international, www.sciencedomain.org, ISSN: 2348-0130, 2015, 11-19.
15. El Naggar M. A. and El Messiery M. A.A Mathematical Model for Pulsating Flow of Ionic Fluid under an Axial Electric Field: EMF Effect on Blood Flow. Journal of Physical Science and Application, JSAP, (2), ISSN 4, 2012, 61-70.
16. Findlay R., Computational Dosimetry and the EMF Directive A presentation for the Health & Safety. World Health Organization, 2013EMFComp, 2006, ISBN 924.
17. Smith D., Electromagnetic characterization through and around human body by simulation using SEMCAD X. 2008, Technical Report summary1: BANESH.
18. Reddy G.N. and Saha S. Electrical and dielectric properties of wet bone as a function of frequency. IEEE Transactions on Biomedical Engineering, Vol. BME.31, No.3, 1984, 296-304.
19. Gabriel C. Gabriel S. Compilation of the dielectric properties of body tissues at RF and microwave frequencies. June 1996, The dielectric properties of body tissues.
20. Gabriel S., Law R.W. Gabriel C. The dielectric properties of biological tissues: Measurement in the frequency range 10Hz to 20GHz. Physics in medicine and biology, (41), Issn.11, 1996, 2251-2269.
21. Duck F. A. Physical properties of tissues: A comprehensive reference book. 1990, Academic press, London.
22. Cararra N. An internet resource for the calculation of the dielectric properties of biological tissues in the frequency range of 10 Hz to 100 GHz. http://niremf.ifac.cnr.it/tissprop.

23. Martinsen O.G., Grimnes S., Schawn H.P. Interface Phenomenon and dielectric properties of biological tissue. 2002, Encyclopedia of surface and colloid science, 2643-2652

24. Faktorova D., Complex Permittivity of Biological Materials at Microwave Frequencies, Measurement Science Review, Vol.7/2007, 12-15.

25. UMEA, IEEE ICES IEEE/ICES TC95/SC4 C95. IEEE Standard for Safety Levels with Respect to Human Exposure to Radio Frequency Electromagnetic Fields, 3 kHz to 300 GHz. Oct. 6 2009, Sweden.

26. ICNIRP guidelines for limiting exposure to time-varying electric, magnetic and electromagnetic fields (up to 300 GHz). 1998, Health physics 74 (4):494-522.

27. International commission on non-ionizing radiation protection, ICNIRP publication – 2009
ICNIRP statement on the: Guidelines for limiting exposure to Time-varying electric, magnetic, and Electromagnetic fields (up to 300 GHz). Health Physics 2009, 97(3): 257-258.

28. Vecchia P., Exposure of humans to electromagnetic fields, Standards and regulations Ann Ist Super Sanità 2007 | Vol. 43, No. 3: 260-267.

Appendix 1

The complex form of the permittivity is given as, $\varepsilon(f)=\varepsilon' - j\varepsilon''$, refractive index, $n(f) = \sqrt{\varepsilon(f)}$. Reflection and transmission coefficients for the i^th layer are:

$$r_{hi}(f) = \frac{\sqrt{\varepsilon_{i+1}(f)}/\sqrt{\varepsilon_i(f)} - \cos\theta_{i+1}/\cos\theta_i}{\sqrt{\varepsilon_{i+1}(f)}/\sqrt{\varepsilon_i(f)} + \cos\theta_{i+1}/\cos\theta_i} \quad t_{h(i-1)}(f) = \frac{2}{\sqrt{\varepsilon_i(f)}/\sqrt{\varepsilon_{i-1}(f)} + \cos\theta_i/\cos\theta_{i-1}} \qquad (3)$$

$$r_{vi}(f) = \frac{1 - \sqrt{\varepsilon_{i+1}(f)}\cos\theta_{i+1}/\sqrt{\varepsilon_i(f)}\cos\theta_i}{1 + \sqrt{\varepsilon_{i+1}(f)}\cos\theta_{i+1}/\sqrt{\varepsilon_i(f)}\cos\theta_i} \quad t_{v(i-1)}(f) = \frac{2}{1 + \sqrt{\varepsilon_i(f)}\cos\theta_i/\sqrt{\varepsilon_{i-1}(f)}\cos\theta_{i-1}} \qquad (4)$$

$$E_{yi}(x,t) = E_{0i} \times e^{i(2\pi ft - k_i x)} \quad (5)$$

$$H(x,t) = \sqrt{\mu_1(f)\varepsilon_1(f)}E_{0i} \times e^{i(2\pi ft - k_i x)} \quad (6)$$

Where the suffix i , $i-1$ and $i+1$ denote current, preceding and succeeding layers respectively. The incident polarized electric field is assumed to be propagating in the *x*-direction making an angle θ_1 with the normal to the interface surface.

The anterior bone layer is denoted as layer *1*, the bone marrow as layer *2*, and the posterior bone layer as *3*. At the interface from air to layer1, the electric field has two components, horizontal and parallel to the interface, while the magnetic field has only one horizontal component. To avoid redundancy of equations, the transmitted and reflected components of the electromagnetic field through layer *2* are:

$$E_{th2}(x,t) = t_{h1}(f)\, t_{h2}(f)\, E_0\, e^{-\delta 1(f)\frac{\Delta x1}{2} + i(2\pi ft - k_2 x + k_1 \Delta x1)} \qquad (7)$$

$$E_{rh2}(x,t) = t_{h1}(f)\, t_{h2}(f)\, r_{h2}(f) E_0\, e^{-\delta 1(f)\frac{\Delta x1}{2} - \delta 2(f)\frac{\Delta x2}{2} + i(2\pi ft + k_2 x + k_1 \Delta x1 + \pi)} \qquad (8)$$

$$H_{th2}(x,t) = t_{h1}(f)\, t_{h2}(f)\sqrt{\mu_2(f)\varepsilon_2(f)}E_0\cos(\theta_{t2})e^{-\delta 1(f)\frac{\Delta x1}{2}+i(2\pi ft-k_2x+k_1\Delta x1)} \quad (9)$$

$$H_{rh2}(x,t) = t_{h1}(f)\, t_{h2}(f)\, r_{h2}(f)\sqrt{\mu_2(f)\varepsilon_2(f)}E_0\cos(\theta_{r2})\, e^{-\delta 1(f)\frac{\Delta x1}{2}-\delta 2(f)\frac{\Delta x2}{2}+i(2\pi ft+k_2x+k_1\Delta x1+\pi)} \quad (10)$$

$$H_{tv2}(x,t) = t_{v1}(f)\, t_{v2}(f)\sqrt{\mu_2(f)\varepsilon_2(f)}\, E_0\sin(\theta_{t2})\, e^{-\delta 1(f)\frac{\Delta x1}{2}+i(2\pi ft-k_2x)} \quad (11)$$

$$H_{rv2}(x,t) = t_{v1}(f)\, t_{v2}(f)\, r_{v2}(f)\sqrt{\mu_2(f)\varepsilon_2(f)}E_0\sin(\theta_{r2})\; e^{-\delta 1(f)\frac{\Delta x1}{2}-\delta 2(f)\frac{\Delta x2}{2}+i(2\pi ft+k_2x+k_1\Delta x1+\pi)} \quad (12$$

Where δ_1 (f) and δ_2 (f) are the absorption coefficients, $k_1(f)$ and $k_2(f)$ are wave numbers of the successive media.